

Theoretical study of the magnetization dynamics of nondilute ferrofluids

D. V. Berkov,¹ L. Yu. Iskakova,² and A. Yu. Zubarev²

¹*Innovent Technology Development, Pruessingstrasse 27B, D-07745 Jena, Germany*

²*Ural State University, Lenina Ave 51, 620083 Ekaterinburg, Russia*

(Received 9 October 2008; published 23 February 2009)

The paper is devoted to the theoretical investigation of the magnetodipolar interparticle interaction effect on magnetization dynamics in moderately concentrated ferrofluids. We consider a homogenous (without particle aggregates) ferrofluid consisting of identical spherical particles and employ a rigid dipole model, where the magnetic moment of a particle is fixed with respect to the particle itself. In particular, for the magnetization relaxation after the external field is instantly switched off, we show that the magnetodipolar interaction leads to the increase of the initial magnetization relaxation time. For the complex ac susceptibility $\chi(\omega) = \chi'(\omega) + i\chi''(\omega)$ we find that this interaction leads to an overall increase of $\chi''(\omega)$ and shifts the $\chi''(\omega)$ peak towards lower frequencies. Comparing results obtained with our analytical approach (second order virial expansion) to numerical simulation data (Langevin dynamics method), we demonstrate that the employed virial expansion approximation gives a good qualitative description of the ferrofluid magnetization dynamics and provides a satisfactory quantitative agreement with numerical simulations for the dc magnetization relaxation, up to the particle volume fraction $\phi \sim 10\%$, and for the ac susceptibility, up to $\phi \approx 5\%$.

DOI: [10.1103/PhysRevE.79.021407](https://doi.org/10.1103/PhysRevE.79.021407)

PACS number(s): 82.70.Dd, 75.50.Mm, 64.70.Nd

I. INTRODUCTION

In this paper we study the magnetization dynamics in ferrofluids—colloidally stable suspensions of magnetic single-domain particles in a carrier liquid (in order to prevent aggregation of particles due to the magnetodipolar attraction, ferrofluid particles are covered with the special surfactant layers). Due to the possibility to change physical parameters and control the behavior of a ferrofluid by an externally applied field, such systems are of large interest both for fundamental and applied physics. Ferrofluids are used in many existing technologies and are supposed to be highly promising for a variety of potential technical and medical applications [1].

Experiments demonstrate that magnetodipolar interparticle interaction changes significantly both the equilibrium [2] and dynamical [3] properties of ferrofluids. Theoretical models of dynamical properties of dilute ferrofluids with vanishing interparticle interactions have been proposed in [4–7]. These models lead to very accurate results for very dilute ferrofluids but cannot explain properties and behavior of ferrofluids where the interparticle interaction is significant.

Depending on the energy of this magnetodipolar interaction, it can lead either to an appearance of homogeneous short- and long-range interparticle correlations, or to a formation of chainlike, droplike, and other heterogeneous internal structures [8]. At present there is no general theory allowing us to predict internal structure in nondilute ferrofluids at given experimental conditions. Therefore it is reasonable to consider effects of different internal structures on the dynamical phenomena in ferrofluids separately. Such idealized models can provide better insights into the influence of various structures and factors on the macroscopical properties of ferrofluids. A combination of corresponding idealized models can serve as a basis for constructing theories of real magnetic fluids with typical long-range interparticle correlations,

where also various heterogeneous particle aggregates are present.

However, before considering dynamical properties of a ferrofluid with various particle aggregates, the behavior of a homogeneous system should be properly understood. For this reason, in this paper we present a model of the magnetization relaxation of a homogeneous ferrofluid consisting of identical particles. It is assumed that the magnetic moment of each particle has a constant magnitude and is “frozen” into the particle body, i.e., relaxation of particle moments has the Brownian character. We realize that this model is obviously the oversimplification of real ferrofluids. The problem is not only a more or less broad distribution of geometric and magnetic particle parameters of real ferrofluids (this can be easily included into the approaches used by us) and particle aggregates often present in real systems (such aggregates obviously require a special treatment). A very important physical aspect also is that the intrinsic magnetic anisotropy of an individual ferrofluid particle is finite (and usually not even large compared to the thermal energy and magnetodipolar interaction field), so that the magnetic moment can rotate with respect to the particle itself (so-called Néel relaxation of magnetic moment). It is well known (see, e.g., [1,3]) that for a dilute (noninteracting) system the Néel relaxation is significant only for very small ferroparticles (with typical diameter $d < 10$ nm). However, for the *interacting* system considered here the magnetodipolar interaction may significantly decrease the single-particle energy barrier, leading to a much faster Néel relaxation even for much larger particles. To avoid these difficulties, we have restricted ourselves to the consideration of the system where the particle moment is fixed with respect to the particle itself. We consider the analysis of this simplified model as a mandatory first step for understanding dynamical properties of real ferrofluids.

Magnetization dynamics of the model outlined above is studied both analytically and using numerical simulations. To obtain analytical results with maximal mathematical accuracy, we take into account the magnetodipolar interparticle

interaction using the regular method of virial expansion over the particle concentration. We assume that magnetodipolar interaction energy is less than or of the same order of magnitude as the thermal energy kT . Otherwise particle aggregates must appear in a ferrofluid, which treatment is out of the framework of this paper. Next, in order to focus on the effects of magnetodipolar interaction, we neglect here effects of the hydrodynamical interaction between particles. Effects of this interaction will be considered in a separate publication.

The paper is organized in the following way. In the next section we explain in detail our analytical approach, deriving the governing equation for the macroscopical magnetization dynamics. In Sec. III we present the numerical simulation methodology and justify our choice of the short-range repulsive potential. In Sec. IV we study the effect of the magnetodipolar interparticle interaction, first on the magnetization relaxation after a stepwise (instant) change of the external field, and second on the ac susceptibility of a ferrofluid. Here we calculate corresponding dynamical system behavior and compare results of the analytical approach to numerical simulation studies, establishing the concentration region where the analytical theory provides a quantitatively accurate description of the magnetization dynamics in ferrofluids.

II. ANALYTICAL APPROACH AND BASIC EQUATION FOR THE MAGNETIZATION DYNAMICS

We consider a ferrofluid with volume V containing N identical spherical ferromagnetic particles with the diameter d . The absolute magnitude p_{mag} of the particle magnetic moment $\mathbf{p}_{i,\text{mag}}$ is constant; the moment is “frozen” into the particle body. We introduce the unit vector $\mathbf{m}_i = \mathbf{p}_{i,\text{mag}}/p_{\text{mag}}$ of the magnetic moment of the i th particle and denote the particle radius vector by \mathbf{r}_i .

To calculate the macroscopic characteristics of this system, we must determine the N -particle distribution function $P_N(\mathbf{m}_1, \dots, \mathbf{m}_N, \mathbf{r}_1, \dots, \mathbf{r}_N)$. It can be found by solving the appropriate Fokker-Planck equation, where we have to take into account magnetodipolar interactions between all particles. This corresponding equation is

$$\begin{aligned} \frac{\partial P_N}{\partial t} = & \sum_i \mathbf{I}_i \left(\frac{D_r}{kT} \mathbf{I}_i (U P_N) \right) + \sum_i \nabla_i \left[\left(\frac{D_t}{kT} \nabla_i U \right) P_N \right] \\ & + D_r \sum_i \mathbf{I}_i^2 P_N + D_t \sum_i \nabla_i^2 P_N, \end{aligned} \quad (1)$$

where the summation in Eq. (1) is performed over particles and we have used the standard notation $\mathbf{I}_i = \mathbf{m}_i \times \frac{\partial}{\partial \mathbf{m}_i}$, $\nabla_i = \frac{\partial}{\partial \mathbf{r}_i}$. The potential energy of the system,

$$U = -kT \sum_i (\boldsymbol{\kappa} \cdot \mathbf{m}_i) + \frac{1}{2} \sum_{i \neq j} w_{ij},$$

contains the energy due to the external field (first term), where the reduced field $\boldsymbol{\kappa} = \mu_0 \frac{p_{\text{mag}} \mathbf{H}}{kT}$ is defined via the vacuum permeability μ_0 , and the applied magnetic field \mathbf{H} .

Magnetodipolar interaction energy (the second term in the expression for U) contains pair interaction terms w_{ij} (interaction energy of particles i and j),

$$w_{ij} = \frac{\mu_0}{4\pi} p_{\text{mag}}^2 \frac{(\mathbf{m}_i \cdot \mathbf{m}_j) r_{ij}^2 - 3(\mathbf{m}_i \cdot \mathbf{r}_{ij})(\mathbf{m}_j \cdot \mathbf{r}_{ij})}{r_{ij}^5}$$

where \mathbf{r}_{ij} is the radius vector between the centers of these particles.

Rotational and translational particle diffusion coefficients,

$$D_r = \frac{kT}{6V_p \eta}, \quad D_t = \frac{kT}{3\pi \eta d},$$

are determined by the hydrodynamical (including the non-magnetic shell) particle diameter d , the carrier fluid viscosity η , and the particle volume $V_p = \pi d^3/6$. In solving Eq. (1) we must take into account the condition that the particles cannot overlap: $r_{ij} \geq d$. Equation (1) is a generalization of the Fokker-Planck equation for the orientational distribution function of a single ferromagnetic particle [4], which takes into account the magnetodipolar interparticle interaction and the particle translational diffusion as well.

The Fokker-Planck equation (1) cannot be solved exactly for two reasons. The first one is the well-known problem of statistical physics—interparticle interaction in a many-particle system does not allow (nearly always) us to solve the governing equation for a many-particle distribution function or to calculate the Gibbs statistical integral. The second reason is the purely mathematical difficulty arising by the solution of the Fokker-Planck equation even for the single particle.

In order to overcome the second problem, we use the effective-field approach, suggested in [4], which is a version of the trial function method. According to this approach, we write the function P_N in the form of an equilibrium Gibbs function in some effective magnetic field \mathbf{H}_e , which must be determined, instead of the real field \mathbf{H} . With other words, we postulate the validity of the following equation:

$$\begin{aligned} \sum_i \mathbf{I}_i \left(\frac{D_r}{kT} \mathbf{I}_i (U_e P_N) \right) + \sum_i \nabla_i \left[\left(\frac{D_t}{kT} \nabla_i U_e \right) P_N \right] + D_r \sum_i \mathbf{I}_i^2 P_N \\ + D_t \sum_i \nabla_i^2 P_N = 0, \end{aligned} \quad (2)$$

where

$$U_e = -kT \sum_i (\boldsymbol{\kappa}_e \cdot \mathbf{m}_i) + \frac{1}{2} \sum_{i \neq j} w_{ij}, \quad \boldsymbol{\kappa}_e = \mu_0 \frac{p_{\text{mag}} \mathbf{H}_e}{kT}.$$

Combining Eqs. (1) and (2), we obtain

$$\frac{\partial P_N}{\partial t} = \sum_i \mathbf{I}_i \left(\frac{D_r}{kT} \mathbf{I}_i (\delta \boldsymbol{\kappa} P_N) \right), \quad \delta \boldsymbol{\kappa} = \boldsymbol{\kappa}_e - \boldsymbol{\kappa}. \quad (3)$$

Up to this point all transformations were exact: instead of the unknown function P_N we have introduced the unknown reduced field $\boldsymbol{\kappa}_e$ linked to P_N by the Gibbs formula

$$P_N = Z^{-1} \exp\left(-\frac{U_e}{kT}\right),$$

$$Z = \int \exp\left(-\frac{U_e}{kT}\right) d\mathbf{m}_1 \cdots d\mathbf{m}_N d\mathbf{r}_1 \cdots d\mathbf{r}_N. \quad (4)$$

The crucial assumption of this method is that the effective field does not depend on the vectors \mathbf{m}_i and \mathbf{r}_i and that the components of this field can be found from the equation for the first statistical moment of the function P_N . Note that for dilute ferrofluids this method leads to a very good agreement with experiments and results of computer simulations (see, e.g., [9]). Similar ideas have been successfully used by analyzing rheological properties of ferrofluids with chainlike aggregates [10].

As usual in statistical physics, in a general case interparticle interactions do not allow us to calculate exactly the average values of physical quantities using Eq. (4). From now on we suppose that particle concentration in our system is not high and we use the virial expansion method. In Sec. V we show that this method represents a reasonable approximation when describing dynamical properties of low and moderately concentrated ferrofluids.

It is convenient, first, to average the distribution function P_N over coordinates \mathbf{r}_i of all particles. Introducing the Mayer function $f_{ij} = \exp(-w_{ij}/kT) - 1$ and averaging Eq. (4) over all \mathbf{r}_i , we obtain the averaged N -particle distribution function p_N in the form

$$p_N = \int P_N \prod_i d\mathbf{r}_i = Z^{-1} \exp\left(\boldsymbol{\kappa}_e \cdot \sum_l \mathbf{m}_l\right) \int \prod_{i>j} (1 + f_{ij}) \prod_k d\mathbf{r}_k. \quad (5)$$

Expanding Eq. (5) in a power series in f_{ij} keeping only the first two terms and performing standard transformations, we obtain

$$p_N = \left(\prod_k \psi_k \right) \left(1 - \phi(N-1)G_e + \frac{1}{V} \sum_{i>j} Q_{ij} \right). \quad (6)$$

Here $\phi = NV_p/V$ is the hydrodynamical (including the non-magnetic particle shell) volume concentration of particles and

$$\begin{aligned} \psi_i &= \psi(\mathbf{m}_i) = \frac{\exp(\boldsymbol{\kappa}_e \cdot \mathbf{m}_i)}{z_1}, \\ z_1 &= \int \exp(\boldsymbol{\kappa}_e \cdot \mathbf{m}) d\mathbf{m} = 4\pi \frac{\sinh \kappa_e}{\kappa_e}, \\ Q_{ij} &= \int_{r_{ij}} f_{ij} d\mathbf{r}_{ij}, \quad G_e = \frac{1}{2V_p} \langle \psi_1 \psi_2 Q_{12} \rangle_{12}, \\ \langle \cdots \rangle_{i \dots k} &= \int \cdots \prod_{l=i}^k d\mathbf{m}_l, \quad i, k = 1, \dots, N. \end{aligned}$$

Calculating the integral in the expression for Q_{ij} , we must keep in mind that the result depends on the shape of the (infinite) integration volume [10]. The reason for this is the long-range character of the dipolar interaction. A physically correct way of integration must provide for a system in thermodynamical equilibrium the equality of the magnetic field in the integration volume to the physical field \mathbf{H} in the sample region where interacting particles are situated. For

this reason we must use as the integration volume an infinitely long cylinder directed along the field \mathbf{H} , with the trial (first) particle on the axis of this cylinder, integrating over all positions of the second particle. Technically this means that in the integral for Q_{ij} (see above) we should use a cylindrical coordinate system (ρ, φ, z) with the z axis along \mathbf{H} . First, we must integrate over the z coordinate of the second particle (from $-\infty$ to $+\infty$), then over other coordinates. This integration order has been successfully used in [11] to calculate the ferrofluid equilibrium magnetization.

Unfortunately, the complicated form of the Mayer function makes the analytical calculation of Q_{ij} impossible. Here we restrict ourselves to the situation when the dipolar interaction energy w_{ij} between particles is $w_{ij} \sim kT$ or smaller. Obviously this assumption means that there are no heteroaggregates in the system.

Expanding the Mayer function in a power series in w_{ij} , keeping only the linear terms, and using the method from [11] to calculate of the integral for Q_{ij} , we obtain

$$\begin{aligned} Q_{ij} &= 8\gamma(\mathbf{m}_i \cdot \mathbf{m}_j), \quad G(x) = 4\lambda L^2(x), \\ L(x) &= \coth x - \frac{1}{x}, \quad G_e = G(\kappa_e), \end{aligned} \quad (7)$$

where the interaction parameter $\lambda = \frac{\mu_0 p_{\text{mag}}^2}{4\pi d^3 kT}$ characterizes the ratio of the dipolar interaction energy of two particles at the contact distance d to the thermal energy kT .

Averaging Eq. (3) over the particle positions, we come to an equation identical to Eq. (3) with p_N instead of P_N . Multiplying the resulting equation by \mathbf{m}_1 and averaging over all \mathbf{m}_i , we obtain

$$\frac{\partial \boldsymbol{\mu}}{\partial t} = -D_r \left\langle \mathbf{m}_1 \sum_i \mathbf{I}_i([\delta \boldsymbol{\kappa} \times \mathbf{m}_i] p_N) \right\rangle, \quad \text{with } \langle \cdots \rangle = \langle \cdots \rangle_{1 \dots N}. \quad (8)$$

Here $\boldsymbol{\mu} = \langle \mathbf{m}_1 p_N \rangle$ is the average of the orientation vector \mathbf{m}_1 of the trial particle. The ferrofluid magnetization is

$$\mathbf{M} = n p_{\text{mag}} \boldsymbol{\mu}, \quad n = \frac{N}{V} = \frac{\phi}{V_p}. \quad (9)$$

Using Eqs. (6) and (7) we find [introducing $L_e = L(\kappa_e)$]

$$\boldsymbol{\mu}(\boldsymbol{\kappa}) = \mu_e \mathbf{e}_h, \quad \mu_e = L_e + \frac{N-1}{V} V_p \frac{dG_e}{d\kappa_e}, \quad \mathbf{e}_h = \frac{\mathbf{H}_e}{H_e}, \quad (10)$$

In the thermodynamical limit (the prime means a derivative with respect to κ_e)

$$\mu_e = L_e + \phi \frac{dG_e}{d\kappa_e} = L_e + 8\phi\lambda L_e L_e'. \quad (11)$$

Taking into account that the angular momentum operator \mathbf{I} is anti-Hermitian and using the approximation (6) for p_N , we obtain

$$\left\langle \mathbf{m}_1 \sum_i \mathbf{I}_i([\delta\boldsymbol{\kappa} \times \mathbf{m}_i]_{p_N}) \right\rangle = \langle \xi p_N \rangle = \langle \xi \psi_1 \rangle + \frac{N-1}{V} v[\langle \xi b \psi_1 \rangle_1 - 2G_e \langle \xi \psi_1 \rangle_1], \quad (12)$$

where $\xi = [\mathbf{m}_1 \times [\delta\boldsymbol{\kappa} \times \mathbf{m}_1]]$ and $b = \langle \psi_2 Q_{12} \rangle_2$, and in the thermodynamical limit

$$\left\langle \mathbf{m}_1 \sum_i \mathbf{I}_i([\delta\boldsymbol{\kappa} \times \mathbf{m}_i]_{p_N}) \right\rangle = \langle \xi p_N \rangle = \langle \xi \psi_1 \rangle + \phi[\langle \xi b \psi_1 \rangle_1 - 2G_e \langle \xi \psi_1 \rangle_1]. \quad (13)$$

Combining Eqs. (6), (7), and (13), after simple transformations we have

$$\left\langle \mathbf{m}_1 \sum_i \mathbf{I}_i([\delta\boldsymbol{\kappa} \times \mathbf{m}_i]_{p_N}) \right\rangle = A_e \delta\boldsymbol{\kappa} - B_e (\mathbf{e}_h \cdot \delta\boldsymbol{\kappa}) \mathbf{e}_h, \quad (14)$$

where the functions

$$A_e = A(\kappa_e), \quad B_e = B(\kappa_e) \quad (15)$$

are defined via

$$A(x) = 1 - L(x)/x + 8\phi\lambda[L^2(x) - C(x)]L(x)/x$$

$$B(x) = C(x) + 8\phi\lambda[L^2(x) - C(x)]L(x)/x, \quad C(x) = 1 - 3L(x)/x.$$

Substituting Eq. (14) into Eqs. (8) and (10), we obtain

$$\frac{\partial \boldsymbol{\mu}}{\partial t} = -D_r [A_e \delta\boldsymbol{\kappa} - B_e (\mathbf{e}_h \cdot \delta\boldsymbol{\kappa}) \mathbf{e}_h]. \quad (16)$$

We arrived at a system of equations (10), (11), and (16) for the vectors $\boldsymbol{\mu}$ and $\boldsymbol{\kappa}_e$. For subsequent calculations it is convenient to write this system in the form of a single equation with respect to $\boldsymbol{\kappa}_e$. To this end we employ the fact that $\boldsymbol{\mu} = \mu_e \mathbf{e}_h$ and write

$$\begin{aligned} \frac{\partial \boldsymbol{\mu}}{\partial t} &= J_e \mathbf{e}_h \frac{\partial \kappa_e}{\partial t} + \mu_e \frac{\partial \mathbf{e}_h}{\partial t}, \\ J_e &= \frac{d\mu_e}{d\kappa_e} = L'_e + 8\phi\lambda[(L')^2 + L_e L''_e]. \end{aligned} \quad (17)$$

Substituting Eq. (17) into the first equation of Eq. (16) and writing the scalar product of the result and vector \mathbf{e}_h , we obtain

$$\frac{d\kappa_e}{dt} = \frac{D_r}{J_e} (B_e - A_e) (\mathbf{e}_h \cdot \delta\boldsymbol{\kappa}). \quad (18)$$

Finally, inserting Eq. (19) into Eq. (17) and the result into Eq. (16), we arrive at the equation

$$\frac{d\mathbf{e}_h}{dt} = -D \frac{A_e}{\mu_e} [\delta\boldsymbol{\kappa} - \mathbf{e}_h (\mathbf{e}_h \cdot \delta\boldsymbol{\kappa})]. \quad (19)$$

Equations (18) and (19) form a system of equations for κ_e and \mathbf{e}_h , which can be easily reduced to a single equation,

$$\frac{d\boldsymbol{\kappa}_e}{dt} = -D_r \left[\frac{A_e - B_e}{\kappa_e^2 J_e} (\boldsymbol{\kappa}_e \delta\boldsymbol{\kappa}) \boldsymbol{\kappa}_e + \frac{A_e}{\mu_e} \boldsymbol{\kappa}_e \left(\delta\boldsymbol{\kappa} - \frac{(\boldsymbol{\kappa}_e \cdot \delta\boldsymbol{\kappa})}{\kappa_e} \boldsymbol{\kappa}_e \right) \right]. \quad (20)$$

To find the macroscopical magnetization $\mathbf{M} = n p_{\text{mag}} \boldsymbol{\mu}$, we have to solve Eq. (20) and substitute the result into Eq. (10).

III. NUMERICAL SIMULATIONS METHODOLOGY

Our numerical simulations are based on the Langevin dynamics formalism, where the equations of motion for the relevant degrees of freedom characterizing our system are solved taking into account thermal fluctuations.

For the ferrofluid model considered in this paper (particles with “fixed” magnetic moments, which are not allowed to move with respect to the particles itself) the system of equations for the description of ferrofluid dynamics includes two equations—for the translational and rotational particle motions. For the time scale of interest ($\sim 10^{-6}$ sec) inertial terms can be neglected due to small particle sizes (~ 10 nm) and a substantial carrier fluid viscosity (~ 0.1 Ps) typical for “standard” ferrofluids.

In this approximation the equation for the translational particle motion in a ferrofluid can be simply deduced from the balance between the viscous force $-b \cdot d\mathbf{r}/dt$ and all other forces acting on the i th ferrofluid particle:

$$b_i \frac{d\mathbf{r}_i}{dt} = \nabla(\mathbf{p}_{i,\text{mag}} \cdot \mathbf{H}_i^{\text{dip}}) - \nabla U_i^{\text{rep}} + \mathbf{F}_i^{\text{fl}}. \quad (21)$$

Here b denotes the viscous friction coefficient, which for a spherical particle with the hydrodynamical radius R_{hyd} in a fluid with the viscosity η is $b = 6\pi\eta R_{\text{hyd}}$. The first term on the right-hand side represents the magnetodipolar interaction force $\mathbf{F}^{\text{dip}} = -\nabla U^{\text{dip}} = \nabla(\mathbf{p}_{\text{mag}} \mathbf{H}^{\text{dip}})$ and the second one represents the steric repulsion force $\mathbf{F}^{\text{rep}} = -\nabla U^{\text{rep}}$. This latter force is due to the nonmagnetic shell surrounding the magnetic particle kernel. The choice of the repulsive potential U^{rep} will be discussed in detail below. The third term is a stochastic thermal force \mathbf{F}^{fl} responsible for a translational Brownian motion. This force has δ -functional correlation properties

$$\langle F_{i,\xi}^{\text{fl}}(0) F_{j,\psi}^{\text{fl}}(t) \rangle = 2kT b_i \delta_{ij} \delta_{\xi\psi} \delta(t)$$

in our model, where the hydrodynamic interaction between particles is neglected.

Employing the same approximations, we can write the equation for particle rotational motion as the balance between the viscous torque and all the other torques:

$$\zeta_i \frac{d\mathbf{p}_{i,\text{mag}}}{dt} = -\mathbf{p}_{i,\text{mag}} \times [\mathbf{p}_{i,\text{mag}} \times \mathbf{H}_i^{\text{dip}}] - [\mathbf{p}_{i,\text{mag}} \times \mathbf{T}_i^{\text{fl}}]. \quad (22)$$

Here $\zeta_i = 8\pi\eta R_{\text{hyd}}^3$ is the rotational viscous friction coefficient. The first term on the right-hand side is the torque exerted on the magnetic moment by the magnetodipolar interaction field \mathbf{H}^{dip} . This torque is directly “transferred” on the particle itself due to the “fixed moment” approximation of our model. The random torque \mathbf{T}^{fl} due to the thermal bath fluctuations leads in the Langevin dynamics formalism to the rotational Brownian motion of the particle. If the hydrodynamic interaction is neglected, the components of \mathbf{T}^{fl} have the same simple correlation properties as for the random force \mathbf{F}^{fl} : $\langle T_{i,\xi}^{\text{fl}}(t) T_{j,\psi}^{\text{fl}}(t') \rangle = 2kT \zeta_i \delta_{ij} \delta_{\xi\psi} \delta(t-t')$.

The system of stochastic differential equations (SDE) (21) and (22) is solved by the optimized Bulirsch-Stoer method (see [12] for the description of the basic idea of this algorithm), which converges to the Stratonovich solution of these SDEs.

We have used a cubic simulation cell and employed periodic boundary conditions (PBCs) to avoid demagnetizing effects of the system borders. Methods for the numerical evaluation of the long-range magnetodipolar field \mathbf{H}^{dip} present in both Eqs. (21) and (22) for PBC are discussed in detail in our review [13]. For this study, where a formation of particle aggregates was not expected (the absence of such aggregates was confirmed by simulations), we have chosen the modified Lorentz cavity method. In this method, the field on the given ferrofluid particle from all other particles within the spherical Lorentz cavity was computed using the exact summation. The field from the particles outside the cavity was added as a field $\mathbf{H}_L = (4\pi/3)\mathbf{M}$ of homogeneously magnetized media with the magnetization \mathbf{M} created by such a media inside a spherical cavity. Taking into account that the system is homogeneous, the magnetization at each integration step \mathbf{M} was set to be equal to average instantaneous magnetization of the whole system $\langle \mathbf{M}(t) \rangle$. We have used the cutoff radius of the Lorentz sphere $R_L = 2\langle \Delta r \rangle$, where $\langle \Delta r \rangle$ is the mean interparticle distance. It was checked that further increase of R_L does not affect simulation results within statistical errors. This means that the discontinuities of the forces (arising due to the spherical cutoff) when a ferrofluid particle leaves or enters the Lorentz cavity of the given particle can be neglected.

All results presented below have been obtained for a system of particles with the magnetic core radius $R_{\text{mag}} = 6$ nm, nonmagnetic shell thickness $h = 2$ nm, and the particle material magnetization $M = 400$ G, for which the interaction parameter λ [defined after Eq. (7)] is $\lambda = 0.8$.

The next important methodical question is the choice of the short-range repulsive potential U^{rep} present in Eq. (21). The corresponding issue was discussed in [13] from the “physical” point of view, i.e., considering the plausibility of the choice for U^{rep} as a “representative” for a steric repulsion force acting between surfactant-coated magnetic particles in real ferrofluid. In this particular research, however, we have an additional methodical problem: taking into account that one of the main goals of this study is the comparison between analytical theory and numerical simulations, we have to choose the repulsive potential in such a way that it does not introduce an artificial bias into such a comparison.

The simplest choice which would enable a most straightforward comparison between analytical theory and numerical simulations would be the hard-core potential ($U^{\text{rep}} = 0$ for $\Delta r > 2R_{\text{hyd}}$ and $U^{\text{rep}} = \infty$ for $\Delta r < 2R_{\text{hyd}}$). This choice would exactly correspond to the condition that particles are not allowed to overlap used by the analytical solution of the basic Eq. (1). Unfortunately, the hard-core potential is not differentiable, so that the dynamic equation containing it cannot be solved in a standard way. Instead, the so called “collision-based” algorithms (see [14] for the review of these methods) should be employed, where the evaluation of the next collision time is used to determine the maximal time step and the system behavior after the particle collision. Such an algo-

rithm performs quite well when the hard-core potential only exists in the system under study. However, in the presence of another potential (like the magnetodipolar interaction present in our case), the evaluation of the collision time becomes a delicate matter and the “collision-based” algorithms are known to work very slowly.

For this reason we have chosen several kinds of analytical short-range potentials and tested whether and how the simulation results depend on the kind of U^{rep} . Our first choice was the purely exponential potential $U_1^{\text{rep}}(r) = B \exp[-(r - 2R_{\text{mag}})/h]$. The decay radius of this potential is equal to the nonmagnetic shell thickness h and the amplitude B is chosen to be much larger than the maximal magnetodipolar interaction energy of particles with the interparticle distance equal to the magnetic core diameter: $E_{\text{max}}^{\text{dip}} = (\pi/3)M^2V_{\text{mag}}$ (here M is the particle magnetization and V_{mag} is the volume of the magnetic particle core).

The second potential tested by us was the potential of the screened-Coulomb type,

$$U_2^{\text{rep}}(r) = A_q \frac{\exp(-s/q)}{s}, \quad s = \frac{r - 2R_{\text{mag}}}{h}. \quad (23)$$

Here the constant q controls the screening radius $r_{\text{scr}} = hq$, and the amplitude A_q was chosen so that the repulsion force due to the potential (23) was equal to the maximal magnetodipolar attraction force acting between particles placed at the distance $\Delta r = 2R_{\text{hyd}}$. When the constant q decreases, the screening radius $r_{\text{scr}} \rightarrow 0$, and the amplitude $A_q \rightarrow \infty$ preserving the property that the repulsion force $F_{\text{rep}}(\Delta r = 2R_{\text{hyd}})$ is equal to the maximal magnetodipolar attraction force. In this sense we can say that this repulsive potential converges to the hard-core potential with $R_{\text{core}} = 2R_{\text{hyd}}$ when $q \rightarrow 0$.

Test simulation results for the exponential potential $U_1^{\text{rep}}(r) = B \exp[-(r - 2R_{\text{mag}})/h]$ with $B = 10E_{\text{max}}^{\text{dip}}$ and screened-Coulomb potentials $U_2^{\text{rep}}(r)$ with two very different values of the constant q ($q = 0.5$ and $q = 4.0$) are shown in Fig. 1. Potential dependencies on the interparticle distance for all three potentials are shown in Fig. 1(a). The magnetization time dependencies $m(t)$, computed for these three types of U^{rep} after the initially applied magnetic field $H = 200$ Oe is instantly switched off, are displayed Fig 1(b). One can see that within the statistical simulation errors all the time dependencies for all three potentials fully coincide, thus ensuring the independence of the simulation results on the choice of the short-range potential for our system. This proves that the differences between the analytical theory and numerical simulations observed and discussed below are not due to an improper choice of the short-range repulsive potential in our simulations.

Concluding this discussion, we remind that the question concerning the dependence of the equilibrium ferrofluid behavior on the exact form of short-range repulsion potential was studied analytically in [15] (see also references therein). The main result of this study was that for dilute and moderately concentrated ferrofluid where the three-particle correlations are not very important, the equilibrium magnetization of a homogeneous (without particle aggregates) ferrofluid *does not depend* on the form of this short-range potential.

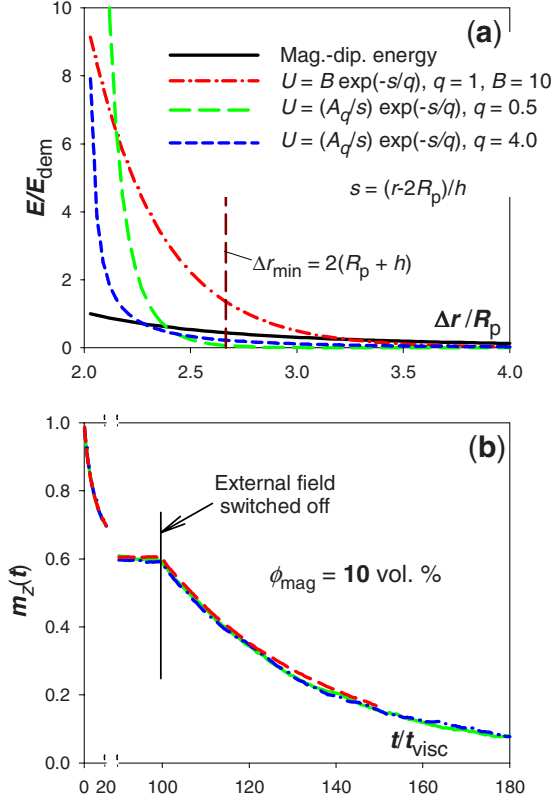


FIG. 1. (Color online) Magnetization relaxation curves after switching the applied field $H=200$ off (at $t/t_{\text{visc}}=100$) for a ferrofluid with the magnetic particle volume fraction $\phi=10\%$ simulated with various short-range repulsion potentials $U(r)$ as shown in the legends. It can be clearly seen that results for various $U(r)$ coincide within statistical errors.

Our numerical simulations show that this conclusion remains true also for the *dynamical* properties of a ferrofluid.

IV. RESULTS AND DISCUSSION

A. Magnetization relaxation after an instantaneous change of an applied field

Let us assume that at the time $t=0$ the magnitude of an applied field changes instantaneously from the initial value H_1 to the final one H_2 , whereby the direction of the field remains the same.

The *analytical approach* outlined above (Sec. II) leads in this case to the following version of the Eq. (20):

$$\frac{d\kappa_e}{dt} = -D_r \left[\frac{A_e - B_e}{J_e} (\kappa_e - \kappa_2) \right] \quad (24)$$

where the initial condition is

$$\kappa_e = \kappa_1 \quad \text{at } t=0 \quad (25)$$

with $\kappa_{1,2} = \mu_0 \rho_{\text{mag}} H_{1,2} / kT$.

The Cauchy problem (24) and (25) can be easily solved with any commercially available software package capable to handle ordinary differential equations.

Numerical simulations of the magnetization dynamics are

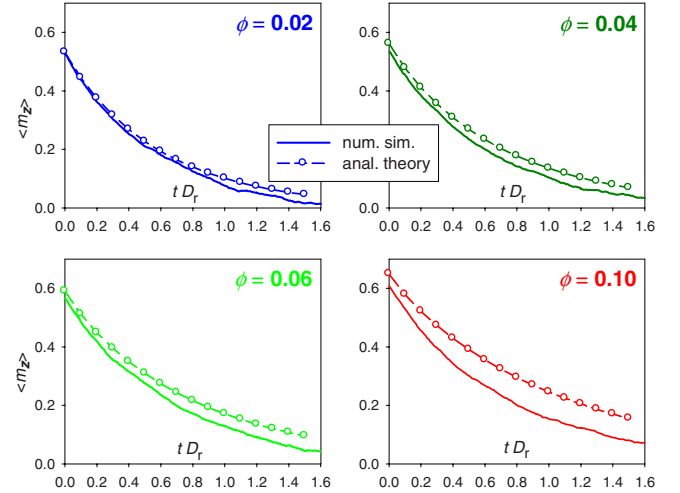


FIG. 2. (Color online) Comparison of the analytical theory (open circles) and numerical simulation results (solid lines): magnetization relaxation $m_z(t)$ after switching off the external field $H=200$ Oe at $t=0$ for various volume fractions of magnetic particles ϕ . Analytical results agree reasonably well with numerical simulation up to the concentration $\phi \approx 6\%$. Note that the disagreement between simulations and analytics is largely due to the difference between the initial (equilibrium) magnetization values $m_{\text{eq}}(H=200)$. Particle parameters: magnetic core radius $R_p=6$ nm, shell thickness $h=2$ nm, magnetization of the core material $M=400$ G.

performed in the following way. We start with the system of particles which magnetic moments are aligned in the direction of the external field \mathbf{H}_1 . The system is equilibrated in this field until the magnetization does not change anymore (in frames of statistical errors); the “annealing” time interval $\Delta t_{\text{ann}} = 5t_{\text{Br}}$ (t_{Br} is the Brownian relaxation time) is usually long enough to achieve this equilibrium. Afterwards, the external field is instantly changed to \mathbf{H}_1 and the magnetization relaxation is recorded. To achieve a high accuracy required, in particular, to determine the relaxation time, we have performed the averaging over $N_{\text{att}}=32$ independent runs for a system of $N_p=1000$ particles.

Corresponding analytical and numerical simulation results are compared for the stepwise decrease and increase of the applied field in Figs. 2 and 4.

For the magnetization decay after the external field is switched off (Fig. 2), one can see that the analytical model agrees with the simulation results fairly well for ferrofluids with concentration of the magnetic phase up to $\phi \approx 6\%$, which represents—from the “applied” point of view—a moderately concentrated ferrofluid. It is interesting to note that the substantial contribution to the disagreement between analytical theory and numerical simulation results from the corresponding disagreement between the initial (equilibrium) magnetization values. The latter is due to the overestimation of the equilibrium ferrofluid magnetization by the second order virial expansion approach.

This important issue is illustrated in Fig. 3, which shows the concentration dependence of the relaxation time defined as

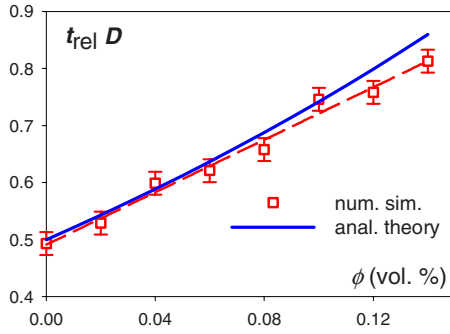


FIG. 3. (Color online) Concentration dependence of the initial relaxation time calculated analytically using the definition Eq. (26) (solid line) and computed numerically from the simulated relaxation curves $m_z(t)$ as described in the text (open squares, dashed line is a guide for an eye). In contrast to relaxation curves, “analytical” and “numerical” initial relaxation times nearly agree (within statistical errors of numerical simulations) up to the highest studied concentration $\phi=14\%$.

$$t_{\text{rel}} = \left| \frac{\langle m_z \rangle}{d\langle m_z \rangle/dt} \right|_{\kappa_e = \kappa_1} \quad (26)$$

after the instant field decrease from $H_1=200$ Oe to $H_2=0$, which corresponds to the initial stage of the relaxation process shown in Fig. 2.

This plot demonstrates, on the one hand, that the magnetic interaction between particles increases the magnetization relaxation time (decreases its relaxation rate) at the initial relaxation stage. In the studied concentration range the increase of t_{rel} is nearly linear with concentration. This increase is caused by the formation of short-range correlation between particle moments; the corresponding correlation degree increases with the particle concentration due to the magneto-dipolar interparticle interaction.

On the other hand, Fig. 3 shows that a good agreement between the analytical model and numerical simulations concerning the *initial* relaxation time persists up to the highest particle volume concentration studied here ($\phi=14\%$, which from the experimental point of view means a highly concentrated ferrofluid), so that the analytical theory predicts this dynamical system feature much better than its equilibrium magnetization value.

The same line of arguments allows us to explain why the agreement between theory and simulations is much better (persists up to higher concentrations) when the external field is initially absent [$H(t=0)=0$] and then is instantly switched on (see Fig. 4). In this case, first of all, the initial (for $t=0$) equilibrium magnetization is, of course, absent [$\mathbf{M}(t=0)=0$] both in analytical theory and simulations. Moreover, one can show analytically that in the second order virial expansion the initial slope of the magnetization curve $dm_z(t)/dt$ does not depend on the particle concentration. Using numerical simulations we have verified that this analytical result is valid up to the highest studied concentration $\phi=14\%$. So for the magnetization *increase* after the external field is switched *on*, the discrepancy between analytical theory and simulation results arises due to the different rate of the magnetization

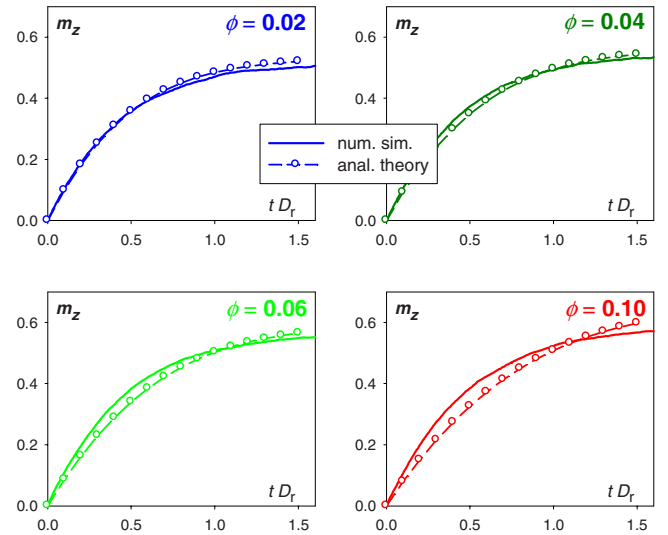


FIG. 4. (Color online) The same as in Fig. 2 for the dc magnetization, when the field $H=200$ Oe is instantly switched on at $t=0$. Particle parameters are the same as in Fig. 2. Note that the agreement between analytical results and numerical simulations is much better than for the $m_z(t)$ relaxation after switching the external field off (compare to the Fig. 2).

change when the system becomes magnetized up to some extent, as can be seen from Fig. 4.

Concluding this subsection, we would like to consider the magnetization relaxation after an instant change of the external field when the effective field κ_e is *nearly equal* to the final field κ_2 ($|\kappa_e - \kappa_2|/\kappa_2 \ll 1$). In this case the relaxation time τ_2 , which characterizes this “linear” magnetization relaxation, exhibits a nontrivial dependence on the final field value κ_2 , as we show below.

In the linear approximation with respect to $\delta\kappa = \kappa_e - \kappa_2$ Eq. (24) can be written as

$$\frac{d\kappa_e}{dt} = -D_r \left[\frac{A_2 - B_2}{J_2} (\kappa_e - \kappa_2) \right], \quad A_2, B_2, J_2 = A, B, J(\kappa_2). \quad (27)$$

One can easily show that in the same approximation Eq. (27) leads to

$$\frac{d\mu}{dt} = -\frac{\mu - \mu_2}{\tau_2}, \quad \text{where } \tau_2 = \frac{1}{D_r} \left[\frac{J_2}{A_2 - B_2} \right], \quad \mu_2 = \mu(\kappa_2) \quad (28)$$

which allows a straightforward calculation of the relaxation time τ_2 .

Corresponding results presenting the relaxation time τ_2 as a function of the final field κ_2 are shown in Fig. 5. One can see that the interaction between particles increases τ_2 (i.e., decreases the relaxation rate) when the field κ_2 is relatively weak and decreases τ_2 (accelerates the magnetization dynamics) when κ_2 is high.

Such a nontrivial dependence of τ_2 on the final field κ_2 is a result of the competition between two factors. The first one is the usual effect of the interparticle interaction, which de-

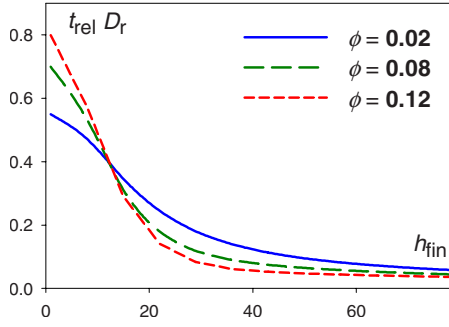


FIG. 5. (Color online) Dependence of the magnetization relaxation time t_{rel} after the instant change of the applied field $H_{\text{init}} \rightarrow H_{\text{fin}}$ on its final value H_{fin} when the initial field H_{init} is only slightly smaller than H_{fin} for various particle concentrations as shown in the legend. Note that the relaxation time t_{rel} increases with the particle concentration ϕ for small final fields $H_{\text{fin}} < 20$, but decreases with ϕ for large fields $H_{\text{fin}} > 20$.

increases the relaxation rate analogous to the magnetization dynamics after a large change of an external field occurs (see above). The second factor is the well known effect of the increase of a mean particle magnetic moment due to the interaction between particles [9,11]. The last factor increases the magnetization relaxation rate. When the final field is weak or moderate, the first factor dominates, when the field is strong, the second one dominates.

B. Complex susceptibility

In this section we study the ferrofluid response to a linearly polarized oscillating field,

$$H_z = H_0 \sin \omega t, \quad H_x = H_y = 0. \quad (29)$$

Analytical approach. Equation (20) now reads

$$\frac{d\kappa_e}{dt} = -D_r \left[\frac{A_e - B_e}{J_e} (\kappa_e - \kappa_0 \sin \omega t) \right], \quad \kappa_0 = \mu_0 \frac{p_{\text{mag}} H_0}{kT}. \quad (30)$$

This equation can be also easily solved numerically. Substituting $\kappa_e(t)$ obtained from Eq. (30) into Eqs. (10) and (11), we find the mean z projection of the moment unit vector $\mu_z(t) \equiv \langle m_z(t) \rangle$. The Fourier transforms

$$\mu'(\Omega) = \int_0^\infty \mu_z(t) \sin(\Omega t) dt, \quad \mu''(\Omega) = \int_0^\infty \mu_z(t) \cos(\Omega t) dt \quad (31)$$

provide the real $\mu'(\Omega)$ and imaginary $\mu''(\Omega)$ parts of μ_ω , related to the corresponding parts of the ferrofluid magnetization Fourier transform as $M_\omega = n p_{\text{mag}} \mu_\omega$. The index ω means here that the applied field oscillates with the frequency ω .

We define the reduced complex susceptibility

$$\chi_{\text{red}}(\omega) = \frac{\mu_\omega(\omega)}{h_0}, \quad (32)$$

where the reduced field is defined via the saturation magnetization of the particle material M_S as $h_0 = H_0 / M_S$. The re-

duced susceptibility (32) is proportional to the standard susceptibility $\chi = M / H_0$ which describes the reaction of the ferrofluid at the same frequency ω as the frequency of the applied field. However, the reduced quantity χ_{red} is more convenient to study the effects of the interparticle interaction, because the trivial proportionality of the standard susceptibility $\chi = M / H_0$ to the particle concentration is eliminated [we remind that $\mu_z(t)$ is the average z projection of the magnetic moment unit vector].

Numerical “measurements” of the complex susceptibility are straightforward and described in detail in our review [13]. In short, we start simulations from the state with chaotically oriented particle magnetic moments and “anneal” the system during $\Delta t_{\text{ann}} = t_{\text{Br}}$ in the absence of an external field. A shorter annealing time—compared to the simulations of the magnetization relaxation described above—is possible, because the average magnetization does not change during the equilibration process, so that only short-range correlations between the particle moments have to be established. Afterwards, we switch on the oscillating field $\mathbf{H} = H_0 \mathbf{e}_z \sin(\omega t)$ and compute the in-phase and out-of-phase responses of the z component of magnetization (L is the number of the time steps). Dividing the results by the field amplitude and by the saturation magnetization of the system [in order to eliminate the proportionality of $\chi = M / H$ to the particle concentration, as by the definition (32)],

$$\begin{aligned} \text{Re}(\chi_{\text{red}}) &\equiv \chi'_{\text{red}} = \frac{1}{h_0} \frac{1}{L} \sum_{l=1}^L \langle m_z(t_l) \rangle \sin(\omega t_l), \\ \text{Im}(\chi_{\text{red}}) &\equiv \chi''_{\text{red}} = \frac{1}{h_0} \frac{1}{L} \sum_{l=1}^L \langle m_z(t_l) \rangle \cos(\omega t_l), \end{aligned} \quad (33)$$

we obtain the complex susceptibility *per particle* χ_{red} . To obtain the frequency dependence of the ac susceptibility at a given temperature $\chi_{\text{red}}(\omega)$, we perform the “measurements” (33) at a set of frequencies sufficiently “dense” to resolve all features of this dependence. To obtain the results with a sufficiently “good” statistics, we have carried out the simulations during $N_{\text{cyc}} = 5$ field cycles at each frequency (so that simulations are especially time consuming in the low-frequency region), and performed the averaging over $N_{\text{att}} = 8$ independent runs for a system with $N_p = 500$ particles each.

Figure 6 demonstrates the comparison of analytical results obtained using Eqs. (30)–(32) and numerical simulations for the real χ'_{red} and imaginary χ''_{red} susceptibility parts. From the qualitative point of view, both the analytical approach and numerical simulations predict the shift of the peak on the imaginary susceptibility part [$\chi''_{\text{red}}(\omega)$ dependence] towards *lower* frequencies with increasing particle volume fraction ϕ . This is in qualitative agreement with the increase of the relaxation time t_{rel} with the growing particle concentration discussed above. Quantitatively, we note that the disagreement between analytical theory and numerical simulations is more significant (for the same particle concentration) than for the magnetization relaxation study performed in the previous subsection. The explanation of this phenomenon can be as

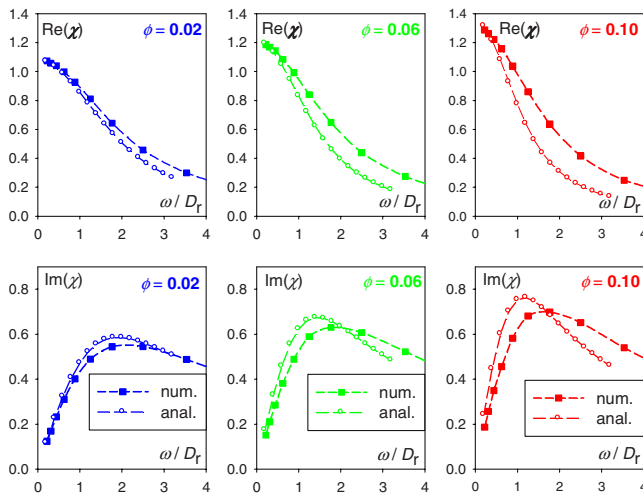


FIG. 6. (Color online) Real (top series) and imaginary (bottom series) parts of the complex susceptibility $\chi(\omega)$ of a ferrofluid with the same particle parameters as on previous figures for three particle concentrations as indicated in the legend. Note that the agreement between numerical results (full squares) and analytical values (open circles) for the susceptibility is significantly worse than for the magnetization relaxation (compare curves on, e.g., Fig. 2 and on this figure for the same particle concentration).

follows. For all concentrations, the deviation between the analytical approach and simulation results for the imaginary part of the ac susceptibility has *different* signs for low and high frequencies (see Fig. 6). Taking into account, that the magnetization relaxation after an instantaneous change of an external field contains contributions from *all* frequencies, the difference between the “analytical” and “numerical” susceptibilities may be partially “averaged out” for the magnetization relaxation process.

V. CONCLUSION

In this paper we have studied the influence of the magnetodipolar interparticle interaction on the magnetization dynamics of a homogeneous ferrofluid using an analytical model and numerical simulations. The analytical model is based on the regular second order virial approximation and does not contain any adjustable parameters or heuristic constructions. It leads to good quantitative agreement with computer simulation results (which can be considered as exact

for our ferrofluid model) up to the volume concentration of magnetic phase, $\phi \sim 5-10\%$, depending on the type of magnetization relaxation under study. We note that these volume concentration can be considered relatively high from the point of view of modern ferrofluid applications.

Our results show that the magnetodipolar interaction increases the characteristic time of the magnetization decay immediately after the applied field is switched off. For the magnetization relaxation for the case when the initial field is close to the final one, the relaxation time demonstrates a more complicated behavior, increasing with the particle concentration if the final field is weak and decreasing if this field is strong. The main effect of the magnetodipolar interaction on the frequency dependence of the ferrofluid ac susceptibility is twofold: this interaction enhances its imaginary part, and shifts the peak on the $\chi''(\omega)$ dependence towards lower frequencies, in accordance with the increase of the system relaxation time mentioned above.

Results presented here are obtained neglecting hydrodynamical interaction between particles. In real ferrofluids the effect of this interaction on the magnetization dynamics can be quite significant. The reasonable agreement between the analytical theory and simulation results for the model without hydrodynamical interaction allows us to consider this system as a basis for the development of models where this interaction is included [13].

Our study of the ferrofluid dynamics has been performed for the “fixed dipole” model, where the particle magnetic moment is fixed with respect to the particle itself. The understanding of this simple model is the necessary first step for the theoretical analysis of this complex system. However, we point out that in order to properly understand the behavior of real ferrofluids, the inclusion of the hydrodynamical interparticle interaction and the extension of the model to allow for the internal magnetic degrees of freedom (rotation of the magnetic moment relative to the particle due to the finite value of the single-particle magnetic anisotropy) is necessary.

ACKNOWLEDGMENTS

This work has been done under the financial support of RFFI, Grants No. 06-01-00125, No. 07-02-00079, No. 07-01-960769Ural, No. 08-02-00647, Fund CRDF, No. PG07-005-02.

[1] R. E. Rosensweig, *Ferrohydrodynamics* (Cambridge University Press, Cambridge, England, 1985).
 [2] A. F. Pshenichnikov, *J. Magn. Magn. Mater.* **145**, 319 (1995); A. F. Pshenichnikov and A. V. Lebedev, *Colloid J.* **57**, 800 (1995).
 [3] J. Zhang, C. Boyd, and W. Luo, *Phys. Rev. Lett.* **77**, 390 (1996); S. Taketomi, *Phys. Rev. E* **57**, 3073 (1998); S. Odenbach, *Magnetoviscous Effects in Ferrofluids* (Springer, New York, 2002).

[4] M. I. Shliomis, *Usp. Fiz. Nauk* **112**, 427 (1974) [*Sov. Phys. Usp.* **17**, 153 (1974)]; M. A. Martsenyuk, Yu. L. Raikher, and M. I. Shliomis, *Zh. Eksp. Teor. Fiz.* **65**, 834 (1973) [*JETP Lett.* **38**, 413 (1974)].
 [5] M. C. Miguel and J. M. Rubi, *Physica A* **231**, 288 (1996).
 [6] J. P. Shen and M. Doi, *J. Phys. Soc. Jpn.* **59**, 111 (1990).
 [7] B. U. Felderhof, *Magnetohydrodynamics* (N.Y.) **36**, 329 (2000).
 [8] C. F. Hayers, *J. Colloid Interface Sci.* **52**, 239 (1975); E. A.

- Peterson and A. A. Krueger, *ibid.* **62**, 24 (1977); J. C. Bacri and D. Salin, *J. Magn. Magn. Mater.* **39**, 48 (1983); A. F. Pshenichnikov, *ibid.* **145**, 319 (1995); P. K. Khizgenkov, V. L. Dorman, and F. G. Barjakhtar, *Magnetohydrodynamics* (N.Y.) **25**, 30 (1989); M. F. Islam, K. H. Lin, D. Lacoste, T. C. Lubensky, and A. G. Yodh, *Phys. Rev. E* **67**, 021402 (2003).
- [9] E. Blums, A. Cebers, and M. Majorov, *Magnetic Fluids* (de Gruyter, Berlin, 1997).
- [10] A. Yu. Zubarev, J. Fleisher, and S. Odenbach, *Physica A* **358**, 475 (2005).
- [11] Yu. A. Buyevich and A. O. Ivanov, *Physica A* **190**, 276 (1992); C. Holm, A. Ivanov, S. Kantorovich, E. Pyanzina, and E. Reznikov, *J. Phys.: Condens. Matter* **18**, S2737 (2006).
- [12] W. H. Press, S. A. Teukolsky, W. T. Vetterling, and B. P. Flannery, *Numerical Recipes in Fortran: the Art of Scientific Computing* (Cambridge University Press, Cambridge, England, 1992).
- [13] D. V. Berkov, N. L. Gorn, R. Schmitz, and D. Stock, *J. Phys.: Condens. Matter* **18**, S2595 (2006).
- [14] M. P. Allen and D. J. Tildesley, *Computer Simulation of Liquids* (Clarendon Press, Oxford, 1993).
- [15] A. O. Ivanov and O. B. Kuznetsova, *Phys. Rev. E* **64**, 041405 (2001).